

## An asymmetric sandpile model with height restriction

This article has been downloaded from IOPscience. Please scroll down to see the full text article.

2009 J. Phys. A: Math. Theor. 42 385003

(<http://iopscience.iop.org/1751-8121/42/38/385003>)

View [the table of contents for this issue](#), or go to the [journal homepage](#) for more

Download details:

IP Address: 171.66.16.155

The article was downloaded on 03/06/2010 at 08:09

Please note that [terms and conditions apply](#).

# An asymmetric sandpile model with height restriction

Evandro F da Silva and Mário J de Oliveira

Instituto de Física, Universidade de São Paulo, Caixa Postal 66318, 05314-970 São Paulo, São Paulo, Brazil

E-mail: [oliveira@if.usp.br](mailto:oliveira@if.usp.br)

Received 6 July 2009

Published 7 September 2009

Online at [stacks.iop.org/JPhysA/42/385003](http://stacks.iop.org/JPhysA/42/385003)

## Abstract

We analyze by numerical simulations and mean-field approximations an asymmetric version of the stochastic sandpile model with height restriction in one dimension. Each site can have at most two particles. Single particles are inactive and do not move. Two particles occupying the same site are active and may hop to neighboring sites following an asymmetric rule. Jumps to the right or to the left occur with distinct probabilities. In the active state, there will be a net current of particles to the right or to the left. We have found that the critical behavior related to the transition from the active to the absorbing state is distinct from the symmetrical case, making the asymmetry a relevant field.

PACS numbers: 05.65.+b, 05.70.Ln, 05.40.-a

(Some figures in this article are in colour only in the electronic version)

## 1. Introduction

Self-organized criticality (SOC) has been successfully described by sandpile lattice models [1–3]. There is a close connection between SOC and stochastic lattice models with infinitely many absorbing states and a nondiffusive conserved field [3–19]. Some of them, which concern us here, are called fixed-energy sandpile models [3, 7, 9, 12, 16, 18]. The conservation law distinguishes these models from other models with infinitely many absorbing states such as the pair contact process [20]. As one increases the density of particles, which represents the nondiffusive conserved field, the lattice models with infinitely many absorbing states display a continuous transition from an absorbing state to an active state. At low densities, the system is trapped in one of the many absorbing states. Above a certain critical density, it is found in an active state with a nonzero density of active sites. The critical behavior places these models into a unique universality class called the Manna universality class, which is distinct from the directed percolation universality class.

**Table 1.** Transition probabilities of the asymmetric model ( $q = 1 - p$ ).

|                       |           |                       |           |
|-----------------------|-----------|-----------------------|-----------|
| 020 $\rightarrow$ 002 | $q^2$     | 120 $\rightarrow$ 102 | $q^2$     |
| 020 $\rightarrow$ 101 | $2pq$     | 120 $\rightarrow$ 201 | $2pq$     |
| 020 $\rightarrow$ 200 | $p^2$     | 120 $\rightarrow$ 210 | $p^2$     |
| 021 $\rightarrow$ 012 | $q^2$     | 121 $\rightarrow$ 112 | $q^2$     |
| 021 $\rightarrow$ 102 | $2pq$     | 121 $\rightarrow$ 202 | $2pq$     |
| 021 $\rightarrow$ 201 | $p^2$     | 121 $\rightarrow$ 211 | $p^2$     |
| 022 $\rightarrow$ 112 | $2pq$     | 220 $\rightarrow$ 202 | $q^2$     |
| 022 $\rightarrow$ 202 | $p^2$     | 220 $\rightarrow$ 211 | $2pq$     |
| 122 $\rightarrow$ 212 | $1 - q^2$ | 221 $\rightarrow$ 212 | $1 - p^2$ |

Among models with infinitely many absorbing states with conserved nondiffusive fields we find the fixed-energy sandpile models [7, 9] which are variants of the Manna model [3]. The Manna model is defined on a lattice in which each site can have any number of particles. A site is considered active if it has two or more particles. At each time step, two particles of an active site jump to neighboring sites. If the number of particles is sufficiently low, the system will eventually be trapped into one of the many absorbing states. However, if the number of particles is sufficiently high, the toppling of particles generates active sites, and the system finds itself in an active state. Here we are concerned with a version of the Manna model in which the maximum height, which is the maximum number of particles in a site, is restricted to 2 [12, 18]. In this restricted version, each site of a lattice can be occupied at most by two particles. A site with two particles is an active site. If a site is empty or has only one particle, it is inactive. At each time step a site is chosen at random. If it is active, one tries to move the two particles to neighboring sites. If the chosen neighboring site has already two particles, the jump is not allowed and the particle remains in the original site.

Specifically we study here an asymmetric version of the height restricted Manna model in one dimension. In this asymmetric version, the jump probability to the right is greater than the jump to the left. This bias implies a net flux of particles to the right. We have found that for any bias there is a continuous transition from an active to a nonactive phase, as expected, but the critical exponents are different from those of the symmetric case. The asymmetry is therefore a relevant property with respect to the critical behavior. The critical exponent related to the order parameter is found to be  $\beta = 1.0$ , and the exponent related to the spatial correlation function is found to be  $\nu_{\perp} = 2.0$ . The quantities used to characterize the critical behavior were obtained by numerical simulations. The phase diagram was obtained by numerical simulations and mean-field approximations.

## 2. Model

Each site of a one-dimensional lattice can be either empty, occupied by just one particle or occupied by two particles. A site having two particles is called active and the two particles are allowed to leave the site. The other sites, empty or with one particle, are inactive. At each time step a site is chosen at random. If it is inactive, the configuration is unchanged. If the chosen site is active, then one attempts to move the two particles to the neighboring sites according to the following rules. One of the particles moves to the left with probability  $p$  and to the right with probability  $q = 1 - p$ . If the chosen neighboring site has already two particles, there is no move. The same procedure is used for the other particle. These rules lead us to the transition probabilities shown in table 1. The asymmetric model is invariant under

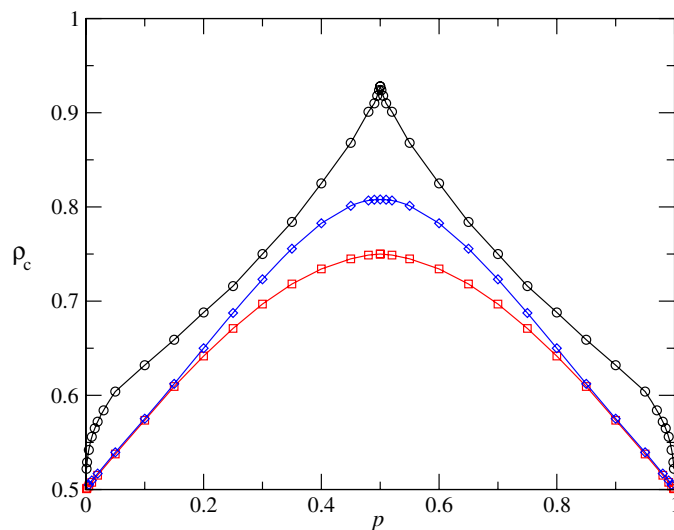


**Figure 1.** Critical line  $\rho_c$  versus  $p$ , obtained from pair mean-field approximation (squares), from three-site mean-field approximation (diamonds) and by numerical simulation and finite-size scaling theory (circles). The active state occurs above the critical line and the absorbing state below it. The critical line obtained from simulation becomes singular at  $p = 0$ ,  $p = 1/2$  and  $p = 1$ .

the operation  $p \rightarrow 1 - p$  and time inversion. It suffices therefore to study the model in the interval  $0 \leq p \leq 1/2$ .

When  $p = 1/2$ , the model is symmetric and corresponds to the *independent* model studied by Dickman *et al* [12] and Dickman [18]. The symmetric model exhibits an active state with nonzero density of active sites  $\rho_a$ , which acts as the order parameter, when the density of particles  $\rho$  is greater than  $\rho_c = 0.9297$ . The asymmetric model,  $p < 1/2$ , behaves similarly but with a critical density of particles  $\rho_c(p)$  that decreases with decreasing values of  $p$  as can be seen in figure 1, reaching the value  $\rho_c = 1/2$  when  $p \rightarrow 0$ .

When  $p = 0$ , that is, when  $p$  is set equal to zero, the system becomes singular and there is no phase transition. In this case, the only allowed transitions, according to table 1, are

$$20 \rightarrow 02 \quad \text{and} \quad 21 \rightarrow 12, \tag{1}$$

each occurring with probability 1. The active number of sites, as well as the number of sites with just one particle, does not change and becomes determined by the initial condition. In fact, as there is no creation or annihilation of active sites, this problem can be regarded as an asymmetric diffusion of three types of particles: 0, 1 and 2. Particles of type 2 can move only to the right. Particles of types 0 and 1 can move only to the left. As a consequence, particles of types 0 and 1 do not exchange places and their relative positions are determined uniquely by the initial configuration.

### 3. Mean-field approximation

Let us denote by  $P_0$ ,  $P_1$  and  $P_2$  the probability of a site being empty, occupied by just one particle and occupied by two particles. The density of particles is  $\rho = P_1 + 2P_2$ , which is a

conserved quantity. Since  $P_0 + P_1 + P_2 = 1$ , we are left with just one independent quantity which we choose to be  $P_0$ . The time evolution of this quantity is given by

$$\frac{d}{dt}P_0 = 2pq\{P_{121} - P_{020} - P_{022} - P_{220}\}, \quad (2)$$

which is valid as long as  $p \neq 0$  and  $p \neq 1$ , where  $P_{xyz}$  denotes the probability of three consecutive sites being in states  $x$ ,  $y$  and  $z$ . Using the simplest mean-field approximation in which  $P_{xyz} = P_x P_y P_z$  we get the equation

$$\frac{d}{dt}P_0 = 2pqP_2\{P_1^2 - P_0^2 - 2P_0P_2\}, \quad (3)$$

which is a closed equation for  $P_0$  since  $P_1 = 2(1 - P_0) - \rho$  and  $P_2 = \rho - (1 - P_0)$ .

In the stationary state, the right-hand side vanishes and it can be solved for  $P_0$ . The solution gives the following result for  $P_2 = \rho_a$ , which is the density of active sites and is regarded as the order parameter,

$$\rho_a = 2 - \sqrt{5 - 2\rho}. \quad (4)$$

The order parameter vanishes continuously at  $\rho = \rho_c = 1/2$ . Near the critical line  $\rho_a \sim (\rho - 1/2)$ , giving an exponent  $\beta = 1$  for the order parameter. We note that the critical line predicted by this mean-field approximation is independent of  $p$ . To remedy this artifact of the simplest mean-field approximation, we will proceed to the pair mean-field approximation.

The pair mean-field approximation involves two-site probabilities  $P_{xy}$  in addition to one-site probabilities  $P_x$ . Of the nine two-site probabilities, five can be determined from the other four, chosen to be  $P_{00}$ ,  $P_{01}$ ,  $P_{10}$ ,  $P_{11}$  and  $P_0$ . The evolution equations for these variables are

$$\frac{d}{dt}P_{00} = (p^2 + q^2)P_{020} - (1 - p^2)P_{200} - (1 - q^2)P_{002}, \quad (5)$$

$$\frac{d}{dt}P_{01} = 2pq(P_{020} + P_{120} + P_{002}) + (p^2 + q^2)P_{021} - (1 - q^2)P_{012} - (1 - p^2)P_{201}, \quad (6)$$

$$\frac{d}{dt}P_{10} = 2pq(P_{020} + P_{021} + P_{200}) + (p^2 + q^2)P_{120} - (1 - q^2)P_{102} - (1 - p^2)P_{210}, \quad (7)$$

$$\begin{aligned} \frac{d}{dt}P_{11} = & 2pq(P_{022} + P_{220} + P_{102} + P_{201}) \\ & + (p^2 + q^2)P_{121} - (1 - q^2)P_{112} - (1 - p^2)P_{211}. \end{aligned} \quad (8)$$

Using the following approximation for the three-site probabilities,  $P_{xyz} = P_{xy}P_{yz}/P_y$ , the above equations together with equation (2) become a closed set of equations for the independent variables  $P_{00}$ ,  $P_{01}$ ,  $P_{10}$ ,  $P_{11}$  and  $P_0$ . The set of closed equations is integrated numerically, and the point where the order parameter  $\rho_a = P_2$  vanishes gives the critical density  $\rho_c$ . The critical line is shown in the phase diagram of figure 1 and now it depends on the parameter  $p$ . The line is smooth and reaches a maximum at  $p = 1/2$  for which  $\rho = 3/4$ . The critical exponent  $\beta = 1$  is the same as the simple mean-field approximation and is independent of  $p$ .

We have also used a three-site mean-field approximation in which the four-site probabilities are written in terms of three- and two-site probabilities, that is,  $P_{xyzw} = P_{xyz}P_{yzw}/P_{yz}$ . After setting up the equations for the three-site probabilities and using this approximation, we have performed a numerical integration and determined the critical density  $\rho_c$  for several values of  $p$ . The critical line determined by using this approximation is shown in figure 1.

We have seen that when  $p \neq 1/2$ , a particle on an active site jumps to the left or to the right with distinct rates. Therefore, we expect that at the stationary state and periodic boundary conditions, there will be a flux of particles to the right or to the left according to whether  $0 \leq p < 1/2$  or  $1/2 < p \leq 1$ , respectively. Using the rates of table 1, it is possible to set up an expression for the particle flux  $\phi$  in terms of two-site probabilities. Consider, for example, the transition coming from the first row of the left panel. Its contribution to the flux will be  $2q^2 P_{020}$  because two particles jump to the right. The contribution coming from the third row of the right panel will be  $-p^2 P_{120}$  because one particle jumps to the left. Using this process we get the following expression:

$$\begin{aligned} \phi = & 2(q - p)P_{020} + 2qP_{220} - 2pP_{022} + (2q^2 - p^2)P_{120} - (2p^2 - q^2)P_{021} \\ & + (1 - p^2)P_{221} - (1 - q^2)P_{122} + (q - p)P_{121}, \end{aligned} \quad (9)$$

which can be written in the simplified form

$$\phi = (q - p)(P_2 - P_{22}) + q^2 P_{20} - p^2 P_{02}. \quad (10)$$

Inserting the stationary solution of any mean-field approximation in this expression, we get the particle flux  $\phi$ . In the simple mean-field approximation

$$\phi = (1 - 2p)(2 - \sqrt{5 - 2\rho})(2 - \rho). \quad (11)$$

In the pair and three-site mean-field approximation, we determined  $\phi$  numerically. Figure 3 shows the result for the three-site approximation. The result (10), which is exact, is also used to calculate  $\phi$  from numerical simulations.

#### 4. Numerical simulations

We have simulated the asymmetric model in lattices of sizes from  $L = 500$  up to  $L = 6000$ , with periodic boundaries starting with a random uncorrelated configuration with  $n$  particles. The simulation was performed according to the rules stated in section 2. We keep a list of active sites from which we choose a site and its first neighbors to be updated at each time step. By using this procedure we avoid wasting computer time by not choosing inactive sites. The time in units of Monte Carlo steps is corrected by an appropriate increase in time. That is, at each updating the time is increased by a value equal to  $n_a^{-1}$ , where  $n_a$  is the number of active sites before the updating step. For each value of the set  $L$ ,  $p$  and  $n$ , we performed from 1000 up to 5000 independent runs. The average values of the interest quantities were obtained by discarding initial configurations, up to time  $t_0$ , and extending each run up to  $t_{\max} = t_0 + t$ . Typical observation times  $t$  were  $10^5$ ,  $2 \times 10^5$ ,  $4 \times 10^5$  Monte Carlo steps. Here we focus on two quantities: the number of active sites and the flux of particles.

For the system defined here, since its length is finite, all initial conditions will eventually drive the system toward an absorbing configuration, if  $n < L$ , even when the expected stationary state is an active state. To overcome this inconvenience, we have slightly changed the dynamics of the model: whenever the system falls into one of the absorbing configurations we create artificially an active site by moving randomly chosen particles to this site. This extra rule will force the system to continue in the active state, even for a small number of particles. This in turn gives rise to an order parameter  $\rho_a = \langle n_a \rangle / L$  which will always be nonzero. However, in the limit  $L \rightarrow \infty$ , the order parameter  $\rho_a$  will vanish if  $p \leq p_c$  and will approach a nonzero value if  $p > p_c$ . This behavior is illustrated in figure 2 which shows  $\rho_a$  as a function of the density of particles  $\rho = n/L$  around the critical point, for  $p = 0.4$ .

The particle flux  $\phi$  was calculated by determining the average numbers of pairs of types 22, 20, 02 and using the exact equation (10). Figure 3 shows  $\phi$  as a function of  $\rho$  for several

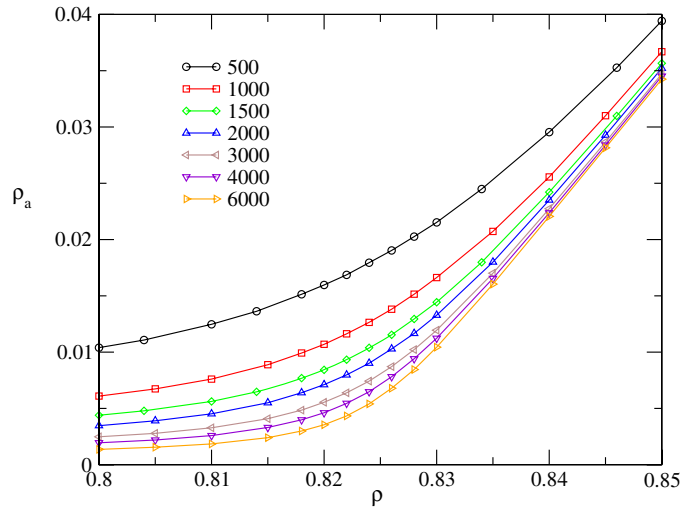


**Figure 2.** Density of active sites  $\rho_a$  versus density  $\rho$  for  $p = 0.4$  and several values of the system size  $L$ . The critical point occurs at  $\rho_c = 0.822(1)$ .

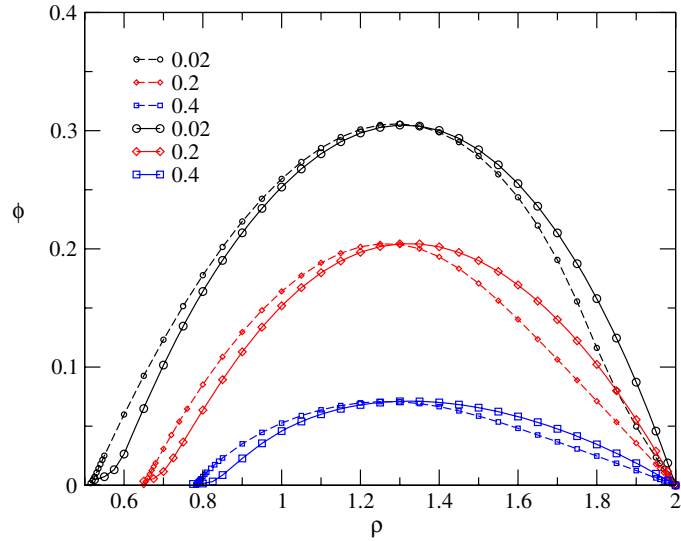


**Figure 3.** Flux  $\phi$  versus density  $\rho$  for several values of the parameter  $p$  as determined from simulations (continuous lines) and the mean-field approximation at the level of three-site approximation (dashed lines).

values of  $p$ . This quantity is nonzero only in the active state and vanishes continuously when  $\rho \rightarrow \rho_c$  and when  $\rho \rightarrow 2$ .

To locate the critical point, we have used two methods. The first is based on the finite-size scaling. For a fixed value of  $p$  we assume the following scaling hypothesis,

$$\rho_a(\rho, L) = L^{-\beta/\nu_\perp} \mathcal{F}(\varepsilon L^{1/\nu_\perp}), \tag{12}$$

where  $\varepsilon = \rho - \rho_c$  and  $\mathcal{F}(x)$  is a universal function. According to this scaling form, when  $\rho = \rho_c$ ,  $\rho_a \sim L^{-\beta/\nu_\perp}$ , implying that  $\ln \rho_a$  behaves linearly with  $\ln L$  when  $\rho = \rho_c$ , with a

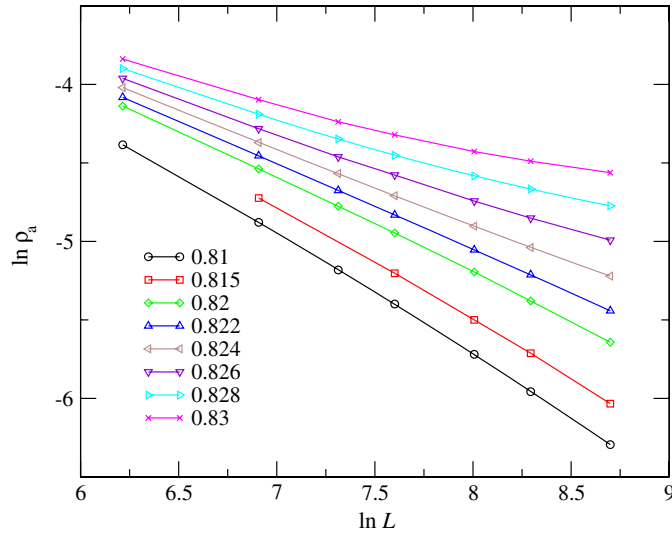


**Figure 4.** Log–log plot of density of active sites  $\rho_a$  versus the system size  $L$  at  $p = 0.4$ , for several values of density  $\rho$ .

slope equal to  $-\beta/\nu_{\perp}$ . From the plot of  $\ln \rho_a$  as a function of  $\ln L$ , for different values of  $\rho$ , the critical point is determined as can be seen in figure 4 for the case  $p = 0.4$ .

In the second method, we use the ratio of moments of different orders. Here we use the ratio

$$m = \frac{\langle n_a^2 \rangle}{\langle n_a \rangle^2}, \tag{13}$$

calculated from different values of  $\rho$  and  $L$ , at constant  $p$ , where  $n_a$  is the number of active sites. At the critical point, the ratio  $m$  is independent of the system size  $L$  [12]. Therefore, a plot of  $m$  versus  $\rho$  for various values of  $L$  shows curves that cross at the critical point, for sufficiently large values of  $L$ . Since the possible values of  $\rho$  form a discrete set, the crossing point is obtained by interpolating cubic splines along the data points.

We used both methods to obtain estimates of the critical point for various values of  $p$ . The lines of critical points determined numerically by both methods coincide within numerical errors and are shown in figure 1. Having determined the location of the critical point, the critical exponents  $\beta$ , related to the critical behavior of the order parameter

$$\rho_a \sim |\rho - \rho_c|^\beta, \tag{14}$$

were obtained by plotting  $\ln \rho_a$  as a function of  $\ln |\rho - \rho_c|$ . We remark that the particle flux  $\phi$  was found to vanish at the critical point with the same critical exponent  $\beta$ . After finding  $\beta$ , we obtained the slope of  $\ln \rho_a$  as a function of  $\ln L$ , at the critical point, which equals  $-\beta/\nu_{\perp}$ , where  $\nu_{\perp}$  is the exponent associated with the spatial correlation length.

The critical exponents  $\beta$  and  $\nu_{\perp}$  are shown in table 2 together with the critical value  $\rho_c$  of the particle density for several values of the parameter  $p$ . The critical exponents have the same value, within the numerical errors, for all values of  $p$  such that  $0 < p < 1/2$ . The same is true for the moment ratio  $m$ . For comparison, the last two rows of table 2 show the critical exponents for the symmetric case. We see that the exponents for the asymmetric case are distinct from the symmetric case even for very small bias. This implies that the



**Table 2.** Critical density  $\rho_c$  and critical exponents  $\beta$  and  $\nu_{\perp}$  for some values of  $p$ . The last column shows the moment ratio  $m$  at the critical point. The results in the last two rows are taken from [12] and [18], respectively.

| $p$  | $\rho_c$     | $\beta/\nu_{\perp}$ | $\beta$   | $m$       |
|------|--------------|---------------------|-----------|-----------|
| 0.01 | 0.56(1)      | 0.45(2)             | 1.08(8)   | 1.23(3)   |
| 0.1  | 0.634(1)     | 0.53(2)             | 1.07(4)   | 1.220(5)  |
| 0.2  | 0.687(3)     | 0.50(2)             | 1.09(9)   | 1.233(4)  |
| 0.3  | 0.748(3)     | 0.50(2)             | 1.07(7)   | 1.238(4)  |
| 0.4  | 0.820(3)     | 0.54(3)             | 1.04(5)   | 1.238(5)  |
| 0.49 | 0.910(1)     | 0.61(5)             | 1.0(1)    | 1.214(7)  |
| 0.5  | 0.929 65(3)  | 0.247(2)            | 0.412(4)  | 1.1596(4) |
| 0.5  | 0.929 780(7) | 0.213(6)            | 0.289(13) | 1.142(8)  |

asymmetry is a relevant field with respect to the critical behavior. For all values of  $p$ , distinct from  $p = 0$ ,  $p = 1/2$  and  $p = 1$ , the exponents are the same and consistent with the values  $\beta = 1.0$  and  $\nu_{\perp} = 2.0$ .

Analyzing the critical line obtained by numerical simulations we see that it is located above the mean-field critical lines. The remarkable result, however, is that the numerical critical line becomes singular at  $\rho = 0$ ,  $\rho = 1/2$  and  $\rho = 1$ , suggesting a nonanalytical behavior around those two points. This singular behavior is confirmed by determining numerically the slope of  $\rho_c$  at these points, which was found to diverge. By assuming the power law behavior around the singular points

$$|\rho_c - \rho_0| \sim |p - p_0|^{\mu}, \quad (15)$$

we found  $\mu = 0.40(1)$  for  $p_0 = 0$  and  $p_0 = 1$  and  $\mu = 0.72(4)$  for  $p_0 = 1/2$ . The nonanalyticity of the critical line at the symmetric point  $p = 1/2$  gives support to the change of universality class at this point.

## 5. Conclusion

We have studied here an asymmetric version of the height restricted Manna model in one dimension in which the jumps of particles to the right and to the left have distinct probabilities. We have found that for any bias there is a continuous transition from an active to a nonactive phase, as happens in the symmetric case. We have found that the critical exponents have the same values along the critical line except that they are distinct from those of the symmetric case. This makes the asymmetry a relevant field with respect to the critical behavior. The critical exponents are found numerically to be  $\beta = 1.0$  and  $\nu_{\perp} = 2.0$ .

## References

- [1] Bak P, Tang C and Wiesenfeld K 1987 *Phys. Rev. Lett.* **59** 381  
Bak P, Tang C and Wiesenfeld K 1988 *Phys. Rev. A* **38** 364
- [2] Dhar D 1990 *Phys. Rev. Lett.* **64** 1613
- [3] Manna S S 1991 *J. Phys. A: Math. Gen.* **24** L363
- [4] Dickman R, Vespignani A and Zapperi S 1998 *Phys. Rev. E* **57** 5095
- [5] Vespignani A, Dickman R, Muñoz M A and Zapperi S 1998 *Phys. Rev. Lett.* **81** 5676
- [6] Dickman R, Muñoz M A, Vespignani A and Zapperi S 2000 *Braz. J. Phys.* **30** 27
- [7] Vespignani A, Dickman R, Muñoz M A and Zapperi S 2000 *Phys. Rev. E* **62** 4564
- [8] Rossi M, Pastor-Satorras R and Vespignani A 2000 *Phys. Rev. Lett.* **85** 1803

- [9] Dickman R, Alava M, Muñoz M A, Peltola J, Vespignani A and Zapperi S 2001 *Phys. Rev. E* **64** 056104
- [10] Lübeck S 2001 *Phys. Rev. E* **64** 016123
- [11] van Wijland F 2003 *Braz. J. Phys.* **33** 551
- [12] Dickman R, Tomé T and de Oliveira M J 2002 *Phys. Rev. E* **66** 016111
- [13] Lübeck S 2002 *Phys. Rev. E* **66** 046114
- [14] de Oliveira M J 2005 *Phys. Rev. E* **71** 016112
- [15] Tomé T and de Oliveira M J 2005 *Phys. Rev. E* **72** 026130
- [16] Dantas W G and Stilck J F 2006 *Braz. J. Phys.* **36** 750
- [17] Fiore C E and de Oliveira M J 2006 *Braz. J. Phys.* **36** 218
- [18] Dickman R 2006 *Phys. Rev. E* **73** 036131
- [19] da Silva E F and de Oliveira M J 2008 *J. Phys. A: Math. Theor.* **41** 385004
- [20] Jensen I and Dickman R 1993 *Phys. Rev. E* **48** 1710